Mannanase A from *Pseudomonas fluorescens* ssp. *cellulosa* Is a Retaining Glycosyl Hydrolase in Which E212 and E320 Are the Putative Catalytic Residues†

David N. Bolam,‡ Neil Hughes,§ Richard Virden,|| Jeremy H. Lakey,|| Geoffery P. Hazlewood,⊥ Bernard Henrissat,▽ Kerynne L. Braithwaite,‡ and Harry J. Gilbert*,‡

Departments of Biological and Nutritional Sciences and Chemistry, University of Newcastle upon Tyne, Newcastle upon Tyne NE1 7RU, U.K., Department of Biochemistry and Genetics, University of Newcastle upon Tyne, Newcastle upon Tyne NE4 4HH, U.K., Department of Cellular Physiology, The Babraham Institute, Babraham, Cambridge CB2 4AT, U.K., and Centre de Recherches sur les Macromoleculécules Végétales, Centre Nationale des Researches Scientifique, BP 53, F-38041 Grenoble cedex 9, France

Received July 29, 1996; Revised Manuscript Received October 9, 1996⊗

ABSTRACT: Mannanase A (MANA) from *Pseudomonas fluorescens*, a member of glycosyl hydrolase family 26, was hyperexpressed in *Escherichia coli* and purified to homogeneity. Analysis of the stereochemical course of mannotetraose hydrolysis by purified MANA showed that the configuration of the anomeric carbon was retained on cleavage of the middle glycosidic bond. These data suggest that the mannanase hydrolyzes mannooligosaccharides by a double-displacement general acid−base mechanism. By hydrophobic cluster analysis (HCA), two glutamate and two aspartate residues were shown to be conserved in all of the glycosyl hydrolase family 26 enzymes analyzed. In addition, HCA suggested that family 26 was related to the GH-A clan (families 1, 2, 5, 10, 30, 35, 39, and 42) of $(\alpha/\beta)_8$-barrel glycosyl hydrolases, which led to the prediction that E320 and E212 constitute the catalytic nucleophile and acid−base residues, respectively. To investigate the role of these amino acids, site-directed mutagenesis was used to replace the two aspartates with alanine and glutamate, while the two conserved glutamates were changed to alanine and aspartate. The mutant enzymes were purified and their biochemical properties were analyzed. The data showed that neither the D → A nor the D → E mutation resulted in a dramatic decrease in enzyme activity, suggesting that the two aspartate residues did not play a pivotal role in catalysis. In contrast, modification of either of the glutamate residues to alanine caused a dramatic decrease in k_{cat} against carob galactomannan, azo-carob galactomannan, mannotetraose and 2,4-dinitrophenyl β-mannobioside (2,4-DNPM). The E320A mutation did not alter the apparent K_m (K_m') of MANA against these substrates, while E212A resulted in a 27-fold decrease in K_m' against 2,4-DNPM. Pre-steady-state kinetics of 2,4-DNPM hydrolysis by E212A showed that there was a rapid burst of 2,4-dinitrophenol release. Circular dichroism and fluorescence spectroscopy indicated that there were no significant differences between the structures of the mutant and wild-type forms of MANA. These data are consistent with E212 and E320 constituting the catalytic acid−base and nucleophile residues of MANA, respectively.

Mannan, one of the major matrix polysaccharides of the plant cell wall, comprises a backbone of β-1,4-linked mannose units which are decorated with galactose and acetate residues, dependent on its origin (Timell, 1967). Endo-β-1,4-mannanases (mannanases) are the major enzymes that cleave the backbone of mannans and glucomannans (McCleary, 1983). The primary sequences of 10 mannanases have now been determined for enzymes from eubacteria (Braithwaite et al., 1995; Gibbs et al., 1992; Arcand et al., 1993; Akino et al., 1989; Mendoza et al., 1995) and anaerobic (Fanutti et al., 1995; Millward-Sadler et al., 1996) and aerobic fungi (Stålbrand et al., 1995; Christgau et al., 1994). Hydrophobic cluster analysis (HCA)[1] and comparison of the primary structures of these enzymes have placed them into two distinct families, namely, families 5 and 26 of glycosyl hydrolases (Henrissat & Bairoch, 1993). Interestingly, both enzyme families contain cellulases, although the catalytic domains of the mannanases analyzed to date do not hydrolyze cellulosic substrates (Millward-Sadler et al., 1996; Ali et al., 1995). Recently, there have been major advances in the elucidation of the three-dimensional structures of a range of cellulases and xylanases, and the identification of the key catalytic residues in these enzymes (Davies & Henrissat, 1995). In contrast, there is a paucity of data on the structure/function relationships of other hemicellulases such as mannanases.

Glycosyl hydrolases can cleave the glycosidic bond via two different mechanisms involving either a single- or a double-displacement reaction. In the former mechanism there is an inversion of configuration about the anomeric

† Financial support was obtained from The Biotechnology and Biological Sciences Reseach Council (Grant LRG13/138) and The Wellcome Trust.

* Corresponding author.

‡ Department of Biological and Nutritional Sciences, University of Newcastle upon Tyne.

§ Department of Chemistry, University of Newcastle upon Tyne.

|| Department of Biochemistry and Genetics, University of Newcastle upon Tyne.

⊥ The Babraham Institute.

▽ Centre de Recherches sur les Macromolécules Végétales, CNRS (affiliated with the Joseph Fourier University, Grenoble, France).

⊗ Abstract published in *Advance ACS Abstracts,* November 15, 1996.

[1] Abbreviations: 2,4-DNP, 2,4-dinitrophenol; 2,4-DNPM, 2,4-dinitrophenyl β-mannobioside; HCA, hydrophobic cluster analysis; K_m', apparent K_m; LB, Luria broth; MANA, mannanase A.

S0006-2960(96)01866-1 CCC: $12.00

carbon, whereas double displacement results in the net retention of the anomeric configuration (Withers, 1995). Recently, Harjunpää et al. (1995) used ^{1}H NMR to show that two *Trichoderma* mannanases, that belong to glycosyl hydrolase family 5, cleaved glycosidic bonds via a double-displacement mechanism. The mode of action of family 26 mannanases remains to be elucidated.

In the active site of glycosyl hydrolases two carboxylic acid residues participate directly in catalysis; a nucleophile and an acid−base catalyst (McCarter & Withers, 1994). Within a specific glycosyl hydrolase family these residues appear to be completely conserved (Henrissat et al., 1995). Several strategies have been employed to identify these residues in a range of glycosidases. X-ray crystallographic determination of the three-dimensional structure of enzyme−substrate (Harris et al., 1994) or enzyme−inhibitor (White et al., 1995) complexes have revealed aspartate and glutamate residues in several glycosyl hydrolases that are in the appropriate location to function as the nucleophile or acid−base catalysts. Identification of the putative catalytic carboxylic acid residues in specific glycosyl hydrolase families has also been achieved using HCA (Henrissat et al., 1995). Mechanism-based inhibitors have been used to trap the glycosyl-enzyme intermediate, enabling the identification of the nucleophile (Wang et al., 1993; Gebler et al., 1992), while affinity labels have been used to probe the location of the acid−base residue (Black et al., 1993). Finally, detailed kinetic analysis of enzymes in which the putative acid−base catalyst has been altered by site-directed mutagenesis has also assisted in the identification of the catalytic residues (MacLeod et al., 1994; Damude et al., 1995).

Although it is now well-established that several mannanases from a diverse range of microorganisms belong to glycosyl hydrolase family 26, the mechanism by which these enzymes cleave their target substrates has not been elucidated, and the two carboxylic acid residues directly involved in catalysis have not been identified. The objective of this report is to determine the mode of action of a family 26 mannanase and to identify its key catalytic amino acids. Data presented in this paper show that mannanase A (MANA) from *Pseudomonas fluorescens* ssp. *cellulosa*, which belongs to glycosyl hydrolase family 26, hydrolyzed mannotetraose by a double-displacement mechanism. HCA identified two aspartate and two glutamate residues that are completely conserved in family 26 enzymes. Analysis of the catalytic properties of mutants of MANA, in which the conserved carboxylic acid residues had been changed to alanine, indicated that E212 and E320 were the acid−base and nucleophile residues, respectively.

MATERIALS AND METHODS

Bacteria, Plasmids, Phage, and Growth Media. The strains of *Escherichia coli* used in this study were JM101 (Vieira & Messing, 1982), JM83, (Norrander et al., 1983), BL21 (Studier & Moffatt, 1986), and the *dut*$^-$ *ung*$^-$ strain CJ236 (supplied by Bio-Rad). The plasmids and bacteriophage used in this study were pKB6 (Braithwaite, 1995), which contains *manA* (encodes full-length MANA) cloned into pET21a, M13mp19 (Vieira & Messing, 1982) and pET21a (Studier & Moffatt, 1986). *E. coli* strains containing recombinant plasmids were cultured in Luria broth (LB) supplemented with 100 μg/mL ampicillin at 37 °C with constant aeration. To select for recombinants expressing mannanase activity, solid media, containing 2% (w/v) agar, were supplemented with 0.05% azo-carob galactomannan. To induce *manA* expression in strains containing the mannanase gene cloned into pET21a, liquid cultures were supplemented with isopropyl β-thiogalactopyranoside (IPTG) to a final concentration of 1 mM.

Recombinant DNA Technology. To select for mutants, DNA was sequenced using the Sequenase version 2.0 kit (Amersham International) employing primers that spanned the appropriate regions of *manA*. To ensure that no unwanted mutations had accumulated during the *in vitro* synthesis of *manA* derivatives, the gene was sequenced using the Prism ready reaction dye-deoxy terminator cycle sequencing kit supplied by Applied Biosystems Instruments (ABI) and the ABI 373 automatic sequencing model. To clone *manA*′ which encoded mature MANA (corresponds to amino acids 39 to 419 of full-length MANA) into the expression vector pET21a, the polymerase chain reaction was used to amplify the appropriate region of *manA*. The 100-μL reactions contained 10 mM Tris/HCl buffer, pH 8.3, containing 50 mM KCl, 2.5 mM $MgCl_2$, 500 μM dNTPs, 200 ng of DNA (pKB6), 250 μM primers, and 2.5 units of DNA polymerase from *Thermus aquaticus* (supplied by Perkin-Elmer). The reactions were overlaid with 50 μL of mineral oil and then subjected to 30 cycles of 1 min at 94 °C, 1 min at 55 °C, and 2 min at 72 °C. The primers used to amplify the region of *manA* between nucleotides 115 and 1257 (*manA*′) that encoded mature mannanase A (amino acids 39−419) were 5′-CTCCATATGAGGGCAGATGTCAAACCTGT-TACG-3′ and 5′-CTCGTCGACTAACTATCAGGGTCG-GACGC-3′. The amplified DNA was restricted with *Nde*I and *Sal*I and cloned into *Nde*I/*Sal*I-digested pET21a to generate pDB1 (contains *manA*′). Site-directed mutagenesis was carried out according to the method of Kunkel (1985). Appropriate mutations were generated by using the following primers to synthesize the DNA *in vitro*: E212D, 5′-ACTGCCGGTATT**A**TCGTGGTACAGG-3′; E212A, 5′-CTGCCGGTATTT**G**CGTGGTACAGGC-3′; D278E, 5′-AAATCCCAGTAC**T**TCCACCCACTCA-3′; D278A, 5′-AATCCCAGTACA**G**CCACCCACTCAT-3′; D283E, 5′-CGGGCCATAGGT**T**TCAAATCCCAGT-3′; D283A, 5′-GGGCCATAGGTAT**G**CAAATCCCAGTA-3′; E320D, 5′-GCGTATACCTAT**G**TCGGAGATCACC-3′; E320D, 5′-CGTATACCTATC**G**CGGAGATCACCG-3′. The mutated nucleotides are in boldface type. The target DNA consisted of a 940-bp *Kpn*I/*Eco*RI restriction fragment of *manA* (nucleotides 270−1210 of full-length *manA*) cloned into *Kpn*I/*Eco*RI-restricted M13mp19. Mutants were identified by sequencing the appropriate regions of *manA*. To ensure that only the desired *manA* mutations had occurred, the complete sequences of *manA* derivatives cloned into M13mp19 were determined. Mutated forms of *manA* were excised from the replicative form of the M13mp19 recombinants by digestion with *Kpn*I and *Eco*RI and cloned into *Kpn*I/*Eco*RI-restricted pDB1. Other recombinant DNA techniques such as agarose gel electrophoresis and elution of DNA from agarose gels were as described by Sambrook et al. (1989).

Enzyme Purification. Native and mutant forms of MANA were purified to homogeneity as follows: Cultures (800 mL) of appropriate recombinant strains of *E. coli* were grown to midexponential phase (A_{600nm} of 0.8), IPTG was added to a final concentration of 1 mM, and the *E. coli* cells were

Table 1: Activity of MANA in Recombinant Strains of *E. coli*[a]

plasmid	mannanase activity (units/mg of total cellular protein)
pKB1	1.1
pKB6	11.2
pDB1	108

[a] The *E. coli* strains were grown to midexponential phase, IPTG was added, and the cells were harvested after a further 2 h. Assays, using azo-carob galactomannan as substrate, were performed on total extracts (contains periplasm, membrane, and cytoplasmic fractions).

Table 2: Cellular Location of MANA

enzyme	plasmid in *E. coli*	enzyme activity in each fraction (%)		
		periplasm	membrane	cytoplasm
MANA	pKB6	70	4	26
MANA	pDB1	98	0	2
β-lactamase	pKB6	89	0	11
β-lactamase	pDB1	96	0	4
NADH ox/red[a]	pKB6	1	81	18
NADH ox/red	pDB1	1	80	19
GPH[b]	pKB6	15	1	84
GPH	pDB1	11	1	88

[a] NADH ox/red = NADH oxidoreductase. [b] GPH = glyceraldehyde-3-phosphate dehydrogenase.

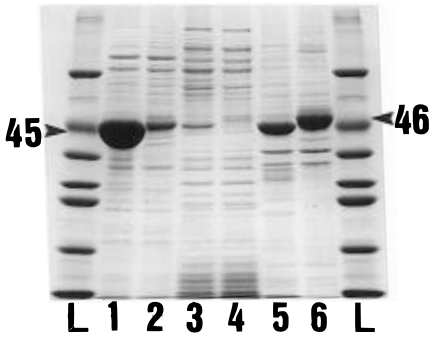

FIGURE 1: SDS−PAGE of the membrane, periplasm, and cytoplasmic fractions of recombinant *E. coli* strains. The periplasmic (lanes 1 and 2), cytoplasmic (lanes 3 and 4), and membrane (lanes 5 and 6) fractions of recombinant strains of *E. coli* harboring pDB1 (lanes 1, 3, and 5) and pKB6 (lanes 2, 4, and 6), respectively, were subjected to SDS−PAGE on a 10% polyacrylamide gel. The prominent polypeptides of M_r 45 000 and 46 000 that correspond to mature MANA and full-length MANA are depicted by 45 and 46, respectively. Sigma low molecular weight standards are shown in lane L.

cultured for a further 2 h. The periplasmic fraction of the recombinant strains, prepared as described by Hall et al. (1989), was applied directly to a 150- × 25-mm DEAE-Trisacryl (Sigma Chemical Co.) column equilibrated with 10 mM Tris-HCl buffer, pH 8.0. Proteins were eluted using a 400 mL linear 0−400-mM NaCl gradient in 10 mM Tris-HCl buffer, pH 8.0. The native and mutant forms of the mannanase were eluted at the same point (100 mM NaCl) in the gradient. The purity of MANA recovered from the ion-exchange column was evaluated by SDS−PAGE as described by Laemmli (1970). Fractions containing pure MANA were dialyzed against 2 × 1000 volumes of 50 mM sodium phosphate buffer, pH 7.0.

Enzyme Assays. The substrates used to assay mannanase activity were obtained from the following sources: carob galactomannan (high viscosity), azo-carob galactomannan, and mannotetraose were purchased from Megazyme Ltd. The synthesis of the substrate 2,4-dinitrophenyl β-mannobioside

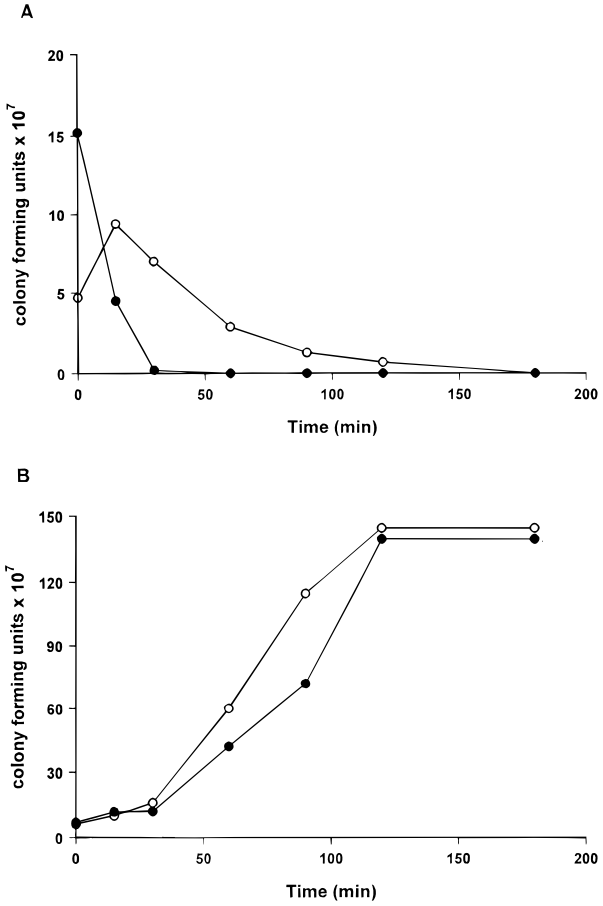

FIGURE 2: Viability of recombinant strains of *E. coli*. The number of colony-forming units in midexponential phase cultures of *E. coli* strains harboring pKB6 (●) and pDB1 (○) 15 min after the addition of IPTG (A) or in the absence of IPTG (B) is plotted.

FIGURE 3: SDS−PAGE of purified MANA. The periplasmic fraction of *E. coli* harboring pDB1 (lane 1), purified wild-type MANA (lane 2), and Sigma molecular weight markers (lane L) were subjected to SDS−PAGE on a 10% polyacrylamide gel.

(2,4-DNPM) will be described elsewhere. Enzyme assays were performed in 50 mM sodium phosphate buffer, pH 7.0, containing 1 mg/mL bovine serum albumin at 37 °C. When 2,4-DNPM was used as the substrate, the generation of the product, 2,4-dinitrophenol (2,4-DNP), was monitored at 400 nm assuming a molar extinction coefficient of 10 356 M^{-1} cm^{-1}. MANA activity against carob galactomannan was determined by measuring the release of reducing sugar as described by Miller (1959). The initial velocity of enzyme reactions was determined over not more than the first 10% of the total reaction, using linear least-squares regression. Each datum was the mean of three determinations. Data were fitted to the Michaelis−Menten equation using non-

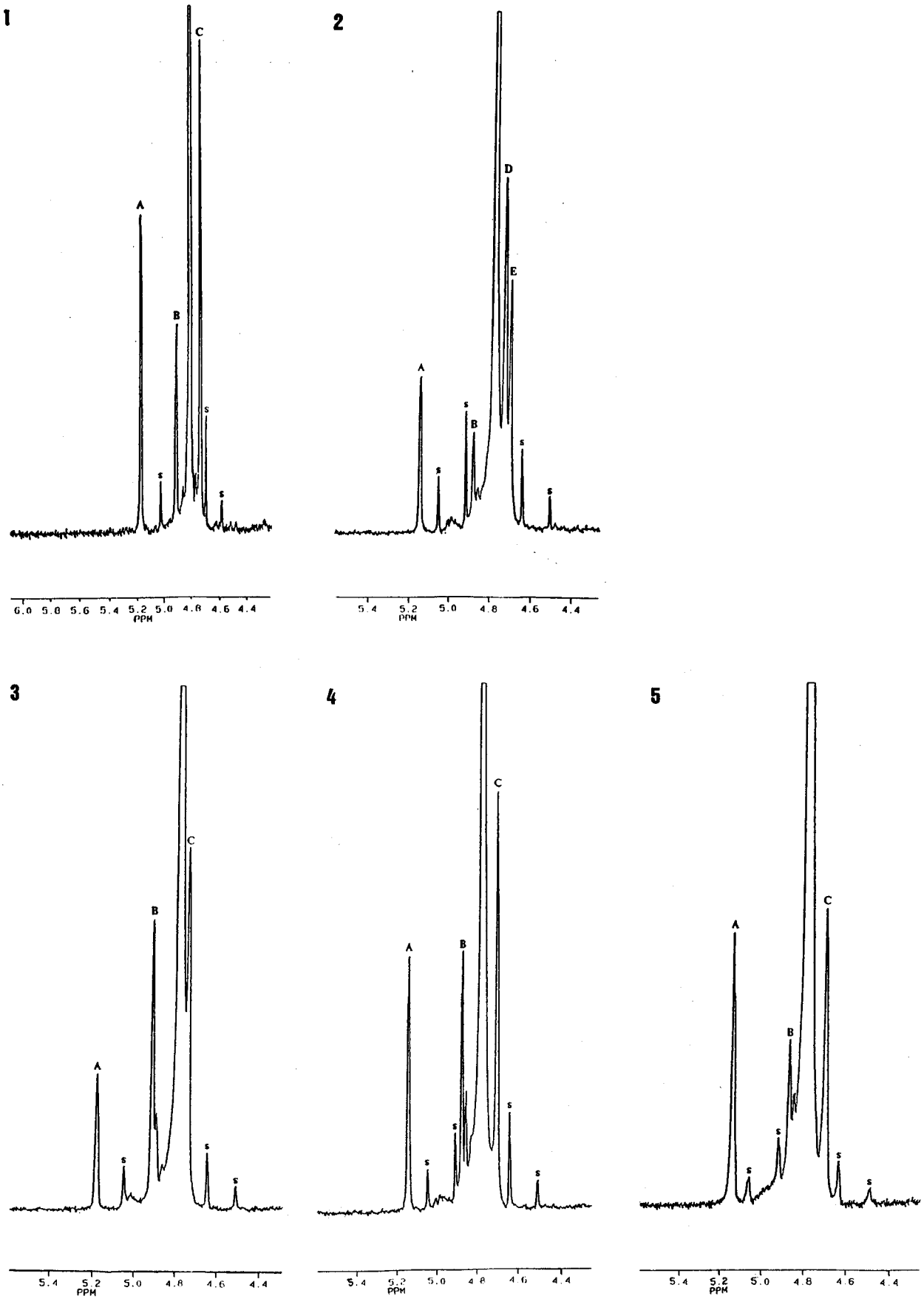

FIGURE 4: ^{1}H NMR analysis of mannotetraose cleavage by MANA. ^{1}H NMR spectra of mannobiose (1), mannotetraose (2), and mannotetraose incubated with MANA for 2 min (3), 30 min (4), and 960 min (5) are shown. The ^{1}H-1α (A), ^{1}H-1β (B) of mannobiose and mannotetraose; ^{1}H-1′ of mannobiose (C); ^{1}H-1′ and ^{1}H-1″(D) and ^{1}H-1‴ (E) of mannotetraose are indicated. Spinning side bands are marked by s.

linear least-squares regression (Duggleby, 1981). The activity of the mannanase against azo-carob galactomannan was assayed as follows: MANA was incubated with 1% of the dyed substrate in a final volume of 500 μL for up to 10 min,

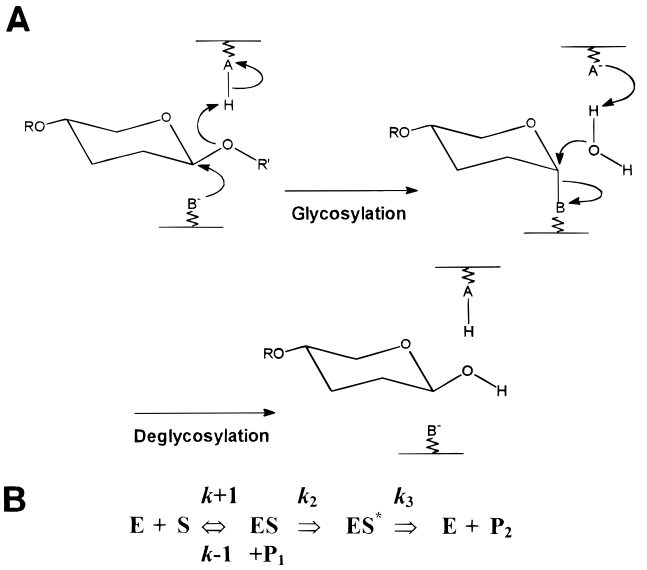

FIGURE 5: Enzymic hydrolysis of a glycosidic bond via a double-displacement acid−base mechanism. Panel A is a schematic of the enzymic hydrolysis of a glycosidic bond by a double-displacement acid−base catalytic mechanism. The B^- and AH residues in the enzyme correspond to the nucleophile and acid−base residues, respectively. Panel B represents a kinetic description of the enzyme mechanism displayed in panel A, where k_2, k_3, E, S, and P represent the rate constant of the glycosylation reaction, the rate constant of the deglycosylation reaction, enzyme, substrate, and product, respectively.

after which time 1 mL of 95% (v/v) ethanol was added and the precipitated substrate was pelleted by centrifugation at 13000*g* for 5 min. The A_{590} of the supernatant was monitored to determine the quantity of dyed oligosaccharides released from the mannan. The rate of hydrolysis of mannotetraose, and the identification of the products generated, were determined by HPLC analysis as described by Braithwaite et al. (1995). Protein concentration of purified MANA was determined by measuring A_{280} following the method of Stoscheck (1990), using a molar extinction coefficient of 93 600 M^{-1} cm^{-1}. The method of Sedmak and Grossberg (1977) was used to measure the protein concentrations of cell-free extracts.

Subcellular Fractionation of E. coli. Periplasmic, membrane, and cytoplasmic fractions of *E. coli* were prepared as described by Hsiung et al. (1986). The purity of the fractions was assessed by assaying for the periplasmic enzyme β-lactamase using the method of Hekman et al. (1990), the membrane-bound enzyme NADH oxidoreductase, and the cytoplasmic enzyme glyceraldehyde-3-phosphate dehydrogenase as described by Minton et al. (1983).

Stereochemical Course of Mannotetraose Hydrolysis. The ^1H NMR spectra were recorded at 200 MHz using a Brucker AC 200 spectrometer. Chemical shifts are given in parts per million (ppm) relative to acetone (2.20 ppm). Mannotetraose was lyophilized twice and then redissolved in D_2O to a final concentration of 25 mM in a 5-mm NMR tube. After the accumulation of the initial spectrum, MANA (10 units), which had been lyophilized and then redissolved in D_2O, was added to the NMR tube, which was immediately placed in the spectrometer probe.

Pre-Steady-State Kinetics. Pre-steady-state kinetics were performed using a stopped-flow apparatus (Applied Photophysics Model SX-17MV), with the flow path thermostatically controlled, and a 10-mm light path to monitor the formation of the product 2,4-DNP at A_{400}. Equal volumes (62.5 μL) of solutions mixed with a dead time of 1.8 ms, contained respectively 2 μM MANA and 16−64 μM 2,4-DNPM in 50 mM sodium phosphate buffer, pH 7.0. The results were analyzed in terms of well-known relationships defining steady-state kinetic parameters and the burst amplitude and kinetics of approach to the steady state (Gutfreund & Sturtevant, 1956).

Circular Dichroism and Fluorescence Spectroscopy. CD spectra were recorded with a Jobin-Yvon CD6 spectropolarimeter. The spectra were obtained at a protein concentration of 10 μM in 50 mM sodium phosphate buffer, pH 7.0, at 25 °C using a 0.1-cm path length quartz cuvette (Hellma .121.000 QS). Each spectrum was accumulated from 20−30 scans between 190 and 250 nm, at a scan rate of 60 nm/min. Fluorescence spectroscopy was performed using a SLM 8100 spectrometer operating in a ratio mode with 8-nm excitation and 4-nm emission bandwidths. Proteins were diluted in 50 mM sodium phosphate buffer, pH 7.0, to a final concentration of 500 nM. Samples were excited at 280 nm and the emission spectra of the proteins were recorded between 290 and 430 nm at 25 °C. Samples were corrected by subtraction of a buffer blank.

Hydrophobic Cluster Analysis. Sequences were retrieved from Swiss-Prot and EMBL databanks. Postscript HCA plots were produced with the HCA-plot program from Doriane S. A. (Le Chesnay, France) and were subsequently assembled using the Island Draw program from Island Graphics (Hoofddorp, The Netherlands). In the HCA plots, the one-letter code amino acid sequence of a protein is drawn as an unrolled and duplicated longitudal cut of a cylinder, where the residues follow an α-helical pattern. Clusters of contiguous hydrophobic residues are automatically contoured by the program. Proline, glycine, serine, and threonine are represented respectively by the following symbols ★, ♦, ⊡, and □ to facilitate the visual inspection of the plots. Analysis of the plots was conducted following published guidelines (Gaboriaud et al., 1987; Lemesle-Varloot et al., 1990; Henrissat et al., 1995).

RESULTS AND DISCUSSION

Hyperexpression of MANA. To investigate the structure/function relationship of MANA, attempts were made to hyperexpress the enzyme in *E. coli*. Initially, pKB6, which consists of the complete coding region of *manA* cloned into the expression vector pET21a, was transformed into *E. coli* BL21. The level of catalytic MANA produced by cells harboring pKB6 (Table 1) was considerably higher than in recombinant *E. coli* strains containing pKB1, a recombinant plasmid in which *manA* was cloned into pBluescript SK^- in the **opposite** orientation to the vector's *lacP* (Braithwaite *et al.,* 1995). Analysis of the cellular location of MANA in cells containing pKB6 revealed that the enzyme was primarily in the membrane fraction in an inactive form (Table 2; Figure 1). These data suggest that the mannanase is inefficiently secreted through the inner membrane of *E. coli*, and this affected both the viability of the recombinant strain (Figure 2) and the level of mannanase activity.

In view of the inefficient secretion of MANA we inserted a derivative of *manA*, encoding mature MANA lacking the *N*-terminal signal peptide, into pET21a to generate pDB1. *E. coli* cells containing the recombinant plasmid synthesized

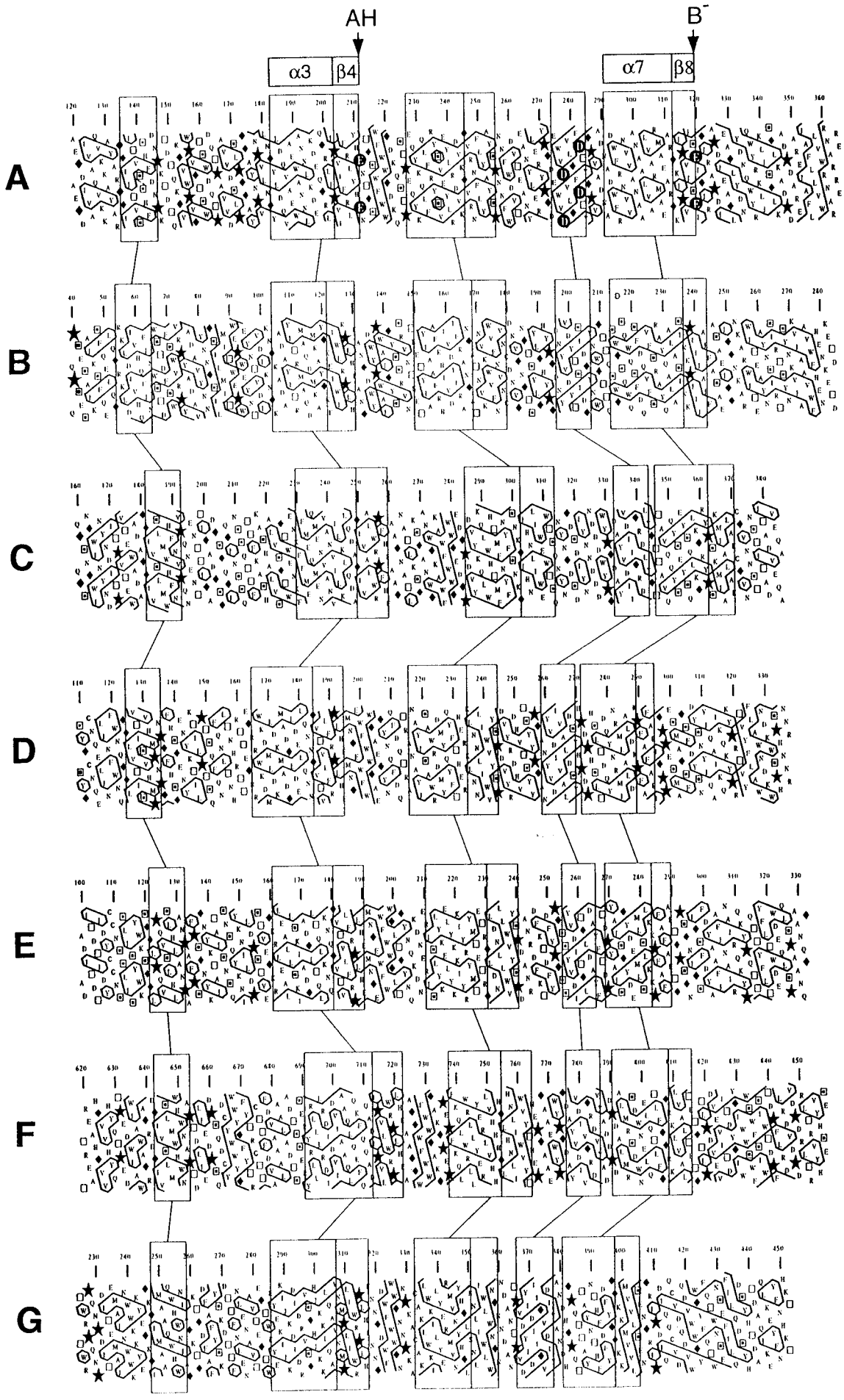
AH
B⁻
α3
β4
α7
β8
A
B
C
D
E
F
G

Table 3: Kinetic Parameters of Wild-Type and Mutant Forms of MANA

enzyme	azo-carob galactomannan (units/mg of protein)	mannotetraose k_{cat} (s^{-1})	2,4 DNPM		carob galactomannan	
			k_{cat} (s^{-1})	K_m' [b] (μM)	k_{cat} (s^{-1})	K_m' [b] (mg/mL)
wild type	270	3861	14.7 ± 0.6	12.3 ± 1.3	1759 ± 118.4	0.90 ± 0.1
E212A	0.05	0.095	0.082 ± 0.006	0.463 ± 0.039	0.04 ± 0.002	0.52 ± 0.04
E320A	0.1	0.060	0.077 ± 0.004	10.8 ± 1.2	0.05 ± 0.003	0.97 ± 0.01
E212D	2.9	0.45	1.24 ± 0.01	2.1 ± 0.142		
E320D	ND[c]	0.04	ND	ND		
D283A	1.8	1.5				
D278A	3.0	1.2				
D283E	86.4	22.5				
D278E	138	807				

[a] Activity against azo-carob galatomannan was measured at only one substrate concentration and thus is a measure of specific activity (micromols of product per minute per milligram of protein) and not k_{cat}. [b] K_m' is the apparent K_m. [c] ND, no catalytic activity detectable.

very high levels of functional mannanase (Table 1) which, surprisingly, was located in the periplasm (Table 2 and Figure 1). Although unusual, the secretion of proteins that lack an ***N***-terminal signal peptide through the inner membrane of *E. coli* has been reported previously (Hall et al., 1989; Soole et al., 1993). These proteins generally contain an internal hydrophobic sequence that is capable of forming an α-helix (Saier et al., 1989). Inspection of the MANA sequence revealed a similar hydrophobic regions between residues 178−185 and 227−236 of the mature enzyme (Braithwaite *et al.*, 1995). It is not apparent why the derivative of MANA lacking an ***N***-terminal signal peptide, and not full-length MANA, should be efficiently secreted through the *E. coli* membrane. It is possible that the **N**-terminal signal peptide of MANA is poorly recognized by the *E. coli* signal peptidase, causing the enzyme to become trapped in the membrane.

Catalytic Mechanism of MANA. To investigate the catalytic mechanism of MANA, the enzyme was purified from cells containing pDB1 (Figure 3) and incubated with mannotetraose in the presence of D_2O. The stereochemistry of enzymic cleavage of the substrate was monitored by ^1H NMR. The data, presented in Figure 4, showed that the H-1α and H-1β signals for both mannotetraose and mannobiose were at 5.17 and 4.90 ppm, respectively, and in identical ratios (α:β 65:35). The other anomeric signals were as follows: mannobiose, 4.73 ppm (H-1′); mannotetraose, 4.73 ppm (H-1″) and 4.76 ppm (H-1′ and H-1″). These assignments are based on empirical rules for chemical shifts and comparison of the relative intensities of resonances and agree with earlier published data (McCleary et al., 1982; Harjunpää et al., 1995). The addition of MANA initially changed the ratio of the 5.17 and 4.90 ppm peaks from 65:35 to 65:135. However, with time the ratio of the two peaks reverted to 65:35. HPLC analysis showed that mannotetraose was quantitatively converted to mannobiose within the first 2 min of the enzyme reaction (data not shown). These data clearly show that MANA cleaved mannotetraose with net retention of the anomeric configuration at the cleavage point and that the reaction product subsequently underwent mutarotation into the equilibrium mixture of α- and β-mannobiose. The retention of the β-configuration of the anomeric carbon after bond cleavage indicates that MANA cleaves mannotetraose by a double-displacement mechanism (Withers, 1995). In the first phase of the reaction, the glycosidic bond is cleaved by a combination of nucleophilic attack of the anomeric carbon and protonation of the glycosidic oxygen, generating a glycosyl-enzyme intermediate. In the second stage of the reaction, the enzyme−substrate complex is hydrolyzed by water attacking the anomeric carbon of the glycosyl group (Figure 5).

Analysis of the stereochemical course of reactions catalyzed by a range of glycosyl hydrolases has shown that the mechanism of bond cleavage is conserved in enzymes belonging to the same glycosyl hydrolase family (Gebler et al., 1992). Thus, as MANA belongs to family 26, the data presented above indicates that all enzymes in this family hydrolyze glycosidic bonds via a double-displacement mechanism.

HCA and the Identification of Conserved Acidic Residues in Glycosyl Hydrolase Family 26. The key catalytic amino acids in glycosidases are two carboxylic acid residues, one of which functions as the acid−base and the other as the nucleophile (Davies & Henrissat, 1995). These residues are invariant in enzymes from the same glycosyl hydrolase family. To identify the amino acids directly involved in catalysis in MANA, HCA plots of all family 26 enzymes members were drawn and searched for strictly conserved aspartate and glutamate residues. HCA was used because of its high reliability at high sequence divergence and its ability to detect secondary structure elements (Woodcock et al., 1992). The data, summarized in Figure 6, revealed that only four invariant residues were conserved in family sequences, E212, D278, D283, and E320, indicating that two of these residues could be catalytic. Careful inspection of the HCA plots of family 26 also showed that the 30-residue region preceding each of the invariant glutamates displayed clusters with shapes compatible with a helix followed by a strand (Lemesle-Varloot et al., 1990). These sequence motifs are strikingly similar to those identified in glycosyl hydrolase

FIGURE 6: HCA of family 26 glycosyl hydrolases. The enzymes compared were as follows: A, MANA of *P. fluorescens*; B, N-terminal domain of *Clostridium thermocellum* endoglucanase H; C, open reading frame of *Bacteroides ruminocola*; D, β-mannanase of *Bacillus* sp.; E, β-mannanase of *Bacillus subtilis*; F, β-mannanase of *Rhodothermus maritimus*; G, MANA of *Piromyces* sp. The boxes in the HCA plots show the best-conserved regions between the enzymes. The residues that were mutated in MANA are shown in white on black circles. The boxes at the top of the figure show the location of α-3, β-4, α-7, and β-8 secondary structure elements in the $(\alpha/\beta)_8$ barrel structures of the GH-A clan [see, for example, Ducros et al. (1995)]. These regions were used to fingerprint this clan (Henrissat et al., 1995). Proline, glycine, serine, and threonine are represented respectively by the following symbols ★, ♦, ⊡, and □ to facilitate the visual inspection of the plots. AH and B^- show the location of the catalytic acid−base and nucleophile residues in the GH-A clan, respectively.

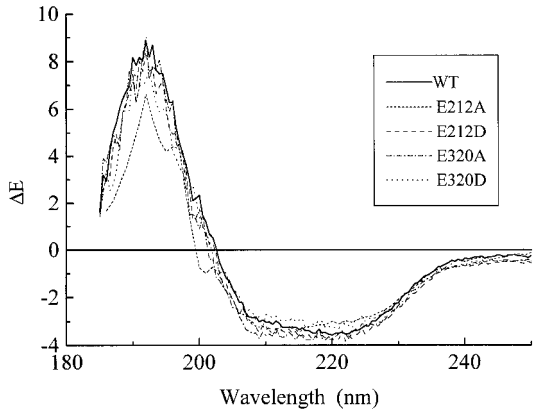

FIGURE 7: CD of wild-type and mutant forms of MANA. Spectra were generated from 10 μM protein samples in a 0.1-cm path length. Between 20 and 30 spectra were collected. The abscissa is represented in units of $\Delta\epsilon$ (M^{-1} cm^{-1}) using the molar concentration of amino acids present. E212A shows a slightly reduced signal amplitude below 195 nm where the signal to noise ratio is poor.

families 1, 2, 5, 10, 17, 30, 35, 39, and 42 (Henrissat et al., 1995). It has been suggested that these nine enzyme families have evolved from a common ancestral sequence that had a $(\alpha/\beta)_8$ barrel structure with the acid−base catalytic glutamate at the **C**-terminal end of strand β-4 and the nucleophilic glutamate at the **C**-terminal end of strand β-7 (Henrissat et al., 1995; Jenkins et al., 1995). These glycosyl hydrolase families are now termed the GH-A "clan" (Henrissat & Bairoch, 1996). In this clan, retention of the anomeric configuration has been found for all the families where stereochemistry of hydrolysis has been studied. Family 26 display HCA plots very similar to those of the GH-A clan except for the fact that the acid−base catalyst is invariably preceeded by an asparagine residue in the GH-A clan and by a histidine in family 26. All other features of the HCA plots of family 26 are compatible with those of the GH-A clan. The resemblance of the HCA plots, and the common retaining mechanism of MANA and the other GH-A clan enzymes, strongly suggests that family 26 is part of the GH-A clan and that E320 and E212 are the nucleophile and acid−base catalysts, respectively.

Site-Directed Mutagenesis of Conserved Carboxylic Residues. To investigate whether E320 and E212 are the key active-site catalytic residues of MANA, site-directed mutagenesis was used to change the four conserved carboxylic acid residues to alanine and either aspartate (E212 and E320) or glutamate (D278 and D283). Mutants of MANA were purified to homogeneity, as judged by SDS−PAGE (data not shown), and the kinetic properties of the enzymes were evaluated. The data, presented in Table 3, showed that derivatives of the mannanase, in which the conserved aspartates had been changed to either glutamate or alanine, retained significant activity against mannotetraose and azocarob galactomannan. In contrast, changing either of the conserved glutamates to alanine or aspartate caused a substantial decrease in the activity of the enzymes. To evaluate whether the substitution of E212 and E320, with either alanine or aspartate, decreased the activity of MANA by influencing the overall structure of the mannanase, native MANA and E212A, E212D, E320A, and E320D mutants were subjected to CD and fluoresence spectroscopy. The CD spectra of the five proteins were essentially identical (Figure 7). Similarly, there was no significant difference in fluoresence spectra of the native and mutant forms of the mannanase (data not shown). These data indicate that E212 and E320 do not play a critical role in maintaining the three-dimensional structure of the enzyme but constitute the key active-site residues of MANA. It is interesting to note that the activity of wild-type MANA against 2,4-DNPM is approximately 150 times lower than against mannan and mannotetraose, while the activity of E212A and E320A against the three substrates was similar. We suggest that the low activity of wild type against 2,4-DNPM reflects the way the molecule sits in the active site; as the substrate interacts with only one of the mannose-binding sites located on either side of E212 and E320, it is possible that the glycosidic bond between the sugar and the chromophore is not in an optimal location to be attacked by E212 and E320. However, in the E212A and E320A mutants, the uniformly low level of remaining catalytic activity is due to factors, other than the key catalytic residues, that contribute to the stabilization of the transition state(s) on the reaction pathway. These other factors contribute equally to the cleavage of the three substrates. Some support for this view is derived from the work of MacLeod et al. (1994) in which the conversion of the acid−base glutamate of a xylanase/exoglucanase to an alanine residue caused a modest reduction in catalytic activity (180-fold) against 2,4-dinitrophenyl β-cellobioside (analagous to 2,4-DNPM) but a 5000-fold decrease for a substrate with a poor leaving group.

Identification of the Nucleophile and Acid/Base Catalyst of MANA. The data above are in agreement with E212 and E320 constituting the key catalytic residues of MANA. However, the results did not establish which amino acid was the nucleophile and which was the acid−base catalyst. To address this question the substrate 2,4-DNPM was synthesized, and the activities of the native and mutant forms of the mannanase against the aryl β-glycoside were evaluated. The data showed (Table 3) that the k_{cat} values of the mutant enzymes were very low compared to that of native MANA. Although the apparent K_m (K_m') of E320A was similar to that of the wild-type mannanase, a large reduction in K_m' was seen with E212A and to a lesser extent with E212D. As the K_m' of E212A against 2,4-DNPM was determined at substrate concentrations above the K_m' (at substrate concentrations lower than the K_m', changes in A_{400} due to 10% substrate hydrolysis were below the sensitivity of the spectrophotometer), the value is likely to be an overestimate of the true K_m value, a view that is supported by the pre-steady-state kinetic data (see below). These results suggest that the rate-limiting step in the hydrolysis of the substrate by E212A is deglycosylation, as a reduction in this step will result in the accumulation of the glycosyl-enzyme intermediate even at low substrate concentrations.

To evaluate the rate-limiting step of 2,4-DNPM hydrolysis, pre-steady-state kinetics of this reaction were analyzed using a stopped-flow apparatus. The data, presented in Figure 8, show the time course of release of 2,4-DNP from 2,4-DNPM, the concentration of which was greater than that of the protein by a factor of 32 and greater than K_m' values for the wild-type, E320A, and E212A enzymes (Table 3) by factors of 2.5, 3.0, and $\geq$70, respectively. The initial rate of release of 2,4-DNP was similar with both wild-type and E212A enzymes, as expected for proteins possessing a catalytic nucleophile, but with the E212A enzyme, which lacks a catalytic acid−base, the rate of release of 2,4-DNP decayed

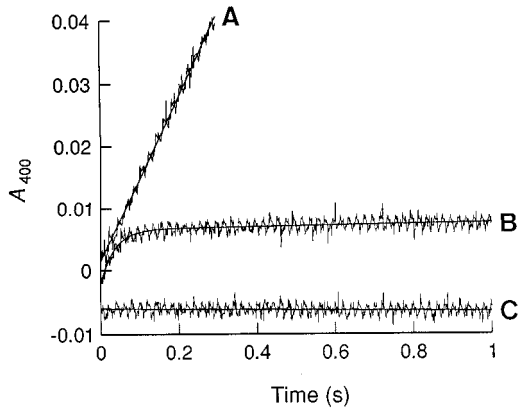

FIGURE 8: Stopped-flow kinetics of 2,4-DNPM hydrolysis by native and mutant forms of MANA. The stopped-flow cell (37 °C) contained 32 μM substrate in 50 mM sodium phosphate buffer, pH 7.0, and 1.0 μM wild-type MANA (A), E212A (B), and E320A (C). Each trace shows data collected at intervals of 1 ms and a continuous line fitted by either linear (wild-type and E320A) or nonlinear (E212A) least-squares regression.

with a first-order constant of 28 s^{-1} leading to a slow steady-state release with a catalytic rate constant of 0.096 s^{-1}. By contrast, the initial rate of release continued with the wild-type enzyme, corresponding to a catalytic rate constant of 8.7 s^{-1}, in reasonable agreement with separately determined steady-state kinetic parameters (Table 3) and with the assumption of a catalytic pathway rate-limited by the k_2 step (Figure 5). The amplitude of the burst with the E212A enzyme was equivalent to 0.8 mol/mol of protein, approaching the value of 1 expected with a saturating substrate concentration and a rate constant for formation of a glycosyl-enzyme intermediate (k_2) considerably greater than for the subsequent hydrolysis of the intermediate (k_3; Figure 5). The rate constant observed for the burst phase was little affected when the substrate concentration was half (16 μM), consistent with a value of k_2 of 30−40 s^{-1} and a value of K_s less than 10 μM. The implied value of 300−400 for the ratio k_2/k_3 suggests a value of K_m of less than 30 nM, at least an order of magnitude less than the experimentally determined maximum steady-state value. With the E320A enzyme, which lacks a catalytic nucleophile, there was no significant pre-steady-state burst of release of 2,4-DNP. These results appear to support the view that deglycosylation is the rate-limiting step in hydrolysis of the aryl β-glycoside by E212A, while glycosylation appears to be the rate-limiting step of 2,4-DNPM cleavage by E320A and native MANA.

The kinetic analysis of the MANA mutants is consistent with the HCA prediction that E320 is the catalytic nucleophile and E212 is the acid−base catalyst of MANA. The rationale for these conclusions are as follows: When MANA hydrolyzes a substrate with a good leaving group, such as 2,4-DNPM (the pK_a of 2,4-DNP is 3.96; Tull & Withers, 1994), protonation of the glycosidic oxygen by the acid−base catalyst is not required for the initial glycosylation step to occur. However, the acid−base residue is required in the hydrolysis of the glycosyl-enzyme intermediate, as it provides base catalytic assistance in the attack of the anomeric carbon by water. Thus, deglycosylation would be the rate-limiting step in the hydrolysis of 2,4-DNPM by a mutant of MANA lacking the acid−base residue, which is consistent with the data obtained for E212A against the aryl β-glycoside.

The nucleophilic residue in retaining glycosyl hydrolases catalyzes the glycosylation step by attacking the anomeric carbon of the substrate. It is apparent, therefore, that glycosylation will be the rate-limiting step of reactions catalyzed by a glycosidase lacking a functional nucleophile, regardless of whether the substrate contains a good leaving group. Thus, the observation that glycosylation is the rate-limiting step in hydrolysis of 2,4-DNPM by E320A (no change in K_m' and no apparent rapid burst of 2,4-DNP release) supports the view that the catalytic nucleophile of MANA is E320.

Conclusions. HCA suggests that glycosyl hydrolase family 26 enzymes belong to the GH-A clan of $(\alpha/\beta)_8$ barrel glycosyl hydrolases and predicts that E212 and E320 constitute the acid−base and nucleophile catalysts of the enzyme, respectively. The prediction is supported by the stereochemical analysis of mannotetraose cleavage by MANA, which showed that the mannanase, in common with the enzymes from the GH-A clan of glycosyl hydrolases, cleaved glycosidic bonds via a retaining mechanism. Kinetic analysis of derivatives of MANA, in which the conserved glutamates have been substituted with either alanine or aspartate residues, provided further support for the view that E212 and E320 were the acid−base and nucleophile catalysts, respectively. Although it could be argued that kinetic analysis alone does not distinguish between the key catalytic amino acids and those residues that play an important role in the function of these amino acids, the view that E212 and E320 are the two catalytic residues of MANA is supported by HCA of the enzyme and by the absence of any other conserved carboxylic acids in glycosyl hydrolase family 26.

REFERENCES

Akino, T., Kato, C., & Horikoshi, K. (1989) *Appl. Environ. Microbiol. 55,* 3178−3183.

Ali, B. R. S., Zhou. L., Graves, F. M., Freedman, R. B., Black, G. W., Gilbert, H. J., & Hazlewood, G. P. (1995) *FEMS Microbiol. Lett. 125,* 15−22.

Arcand, N., Kluepfel, D., Paradis, F. W., Morosoli, R., & Shareck, F. (1993) *Biochem. J. 290,* 857−863.

Braithwaite, K. L. (1995) Ph.D. Thesis, University of Newcastle upon Tyne; U.K.

Braithwaite, K. L., Black, G. W., Hazlewood, G. P., Ali, B. R. S., & Gilbert, H. J. (1995) *Biochem. J. 305,* 1005−1010.

Black, T. S., Kiss, L., Tull, D., & Withers, S. G. (1993) *Carbohydr. Res. 250,* 195−202.

Christgau, S., Kauppinen, S., Vind, J., Kofod, L. V., & Dalbøge, H. (1994) *Mol. Biol. Int. 33,* 917−925.

Damude, H. G., Withers, S. G., Kilburn, D. G., Miller, R. C., Jr., & Warren, R. A. J. (1995) *Biochemistry 34,* 2220−2224.

Davies, G., & Henrissat, B. (1995) *Structure 3,* 853−859.

Ducros, V., Czjzek, M., Belaich, A., Gaudin, C., Fierobe, H.-P., Belaich, J.-P., Davies, G. J., & Haser, R. (1995) *Structure 3,* 939−949.

Duggleby, R. G. (1981) *Anal. Biochem. 110,* 9−18.

Fanutti, C., Ponyi, T., Black, G. W., Hazlewood, G. P., & Gilbert, H. J. (1995) *J. Biol. Chem. 270,* 29314−29322.

Gaboriaud, C., Bissery, V., Benchetrit, T., & Mornon, J.-P. (1987) *FEBS Lett. 224,* 149−155.

Gebler, J. C., Gilkes, N. R., Claeyssens, M., Wilson, D. B., Béguin, P., Wakarchuk, W. W., Kilburn, D. G., Miller, R. C., Warren, R. A. J., & Withers, S. G. (1992) *J. Biol. Chem. 267,* 12559−12561.

Gibbs, M. D., Saul, D. J., Lüthi, E., & Bergquist, P. L. (1992) *Appl. Environ. Microbiol. 58,* 3864−3867.

Gutfreund, H., & Sturtevant (1956) *Biochem. J. 63,* 656−661.

Hall, J., Hazlewood, G. P., Huskisson, N. S., Durrant, A. J., & Gilbert, H. J. (1989) *Mol. Microbiol. 3,* 1211−1219.

Harjunpää, V., Teleman, A., Siika-Aho, M., & Drakenberg, T. (1995) *Eur. J. Biochem. 234,* 278−283.

Harris, G. W., Jenkins, J. A., Connerton, I., Cummings, N., Lo Leggio, L., Scott, M., Hazlewood, G. P., Laurie, J. I., Gilbert, H. J., & Pickersgill, R. W. (1994) *Structure 2*, 1107−1116.
Hekman, W. E., Dennis, D. T., & Miernyk, J. A. (1990) *Mol. Microbiol. 4*, 1363−1369.
Henrissat, B., & Bairoch, A. (1993) *Biochem. J. 293*, 781−788.
Henrissat, B., & Bairoch, A. (1996) *Biochem. J. 316*, 695−696.
Henrissat, B., Callebaut, I, Fabrega, S., Lehn, P., Mornon, J.-P., & Davies, G. (1995) *Proc. Natl. Acad. Sci. U.S.A. 92*, 7090−7094.
Hsiung, H. M., Mayne, N. G., & Becker, G. W. (1986) *Biotechnology 4*, 991−995.
Jenkins, J., Lo Leggio, L., Harris, G., & Pickersgill, R. (1995) *FEBS Lett. 362*, 281−285.
Laemmli, U. K. (1970) *Nature 227*, 680−685.
Lemesie-Varloot, L., Henrissat, B., Gaboriaud, C., Bissery, V., Morgat, A., & Mornon, J.-P. (1990) *Biochimie 72*, 555−574.
MacLeod, A. M., Lindhorst, T., Withers, S. G., & Warren, R. A. J. (1994) *Biochemistry 33*, 6371−6376.
McCarter, J. D., & Withers, S. G. (1994) *Curr. Opin. Struct. Biol. 4*, 885−892.
McCleary, B. V. (1983) *Carbohydr. Res. 119*, 191−219.
McCleary, B. V., Taravel, F. R., & Cheetham, N. W. H. (1982) *Carbohydr. Res. 104*, 285−297.
Mendoza, N. S., Arai, M., Sugimoto, K., Ueda, M., Kawaguchi, T., & Joson, L. M. (1995) *Biochim. Biophys. Acta 1243*, 552−554.
Miller, G. L. (1959) *Anal. Chem. 31*, 426−428.
Millward-Sadler, S. J., Hall, J., Black, G. W., Hazlewood, G. P., & Gilbert, H. J. (1996) *FEMS Microbiol. Lett.* (in press).
Minton, N. P., Atkinson, T., & Sherwood, R. F. (1983) *J. Bacteriol. 156*, 1222−1227.
Norrander, J., Kempt, T., & Messing, J. (1983) *Gene 26*, 101−106.
Saier, M. H., Jr., Werner, P. K., & Müller, M. (1989) *Microbiol. Rev. 53*, 333−366.
Sambrook, J., Fritsch, E. F., & Maniatis, T. (1989) in *Molecular Cloning: A Laboratory Manual* (Ford, N., Ed.) Cold Spring Harbor Laboratory, Cold Spring Harbor, NY.
Sedmak, J. J., & Grossberg, J. R. (1977) *Anal. Biochem. 79*, 544−552.
Soole, K. L., Hirst, B. H., Hazlewood, G. P., Gilbert, H. J., Laurie, J. L., & Hall, J. (1993) *Gene 125*, 85−89.
Stålbrand, H., Saloheimo, A., Vehmaanpera, I., Henrissat, B., & Penttilä, M. (1995) *Appl. Environ. Microbiol. 61*, 1090−1097.
Stoscheck, C. M. (1990) *Methods Enzymol. 182*, 50−68.
Studier, F. W., & Moffatt, B. A. (1986) *J. Mol. Biol. 189*, 113−130.
Timell, T. E. (1967) *Wood Sci. Technol. 1*, 45−70.
Tull, D., & Withers, S. G. (1994) *Biochemistry* 33, 6363−6370.
Vieira, J., & Messing, J. (1982) *Gene 19*, 259−268.
Wang, Q., Tull, D., Meinke, A., Gilkes, N. R., Warren, R. A. J., Aebersold, R., & Withers, S. G. (1993) *J. Biol. Chem. 268*, 14096−14102.
White, A., Tull, D., Johns, K., Withers, S. G., & Rose, D. R. (1995) *Nature Struct. Biol. 3*, 149−154.
Withers, S. G. (1995) in *Progress in Biotechnology Volume 10: Carbohydrate Bioengineering* (Petersen, S. B., Svensson, B., & Pedersen, S., Eds.) pp 97−112, Elsevier, Amsterdam, The Netherlands.
Woodcock, S., Mornon, J.-P., & Henrissat, B. (1992) *Protein Eng. 5*, 629−635.

BI961866D